Molecular Catalysis 463 (2019) 130–139

Contents lists available at ScienceDirect

Molecular Catalysis

journal homepage: www.elsevier.com/locate/mcat

Mechanistic insights on catalytic conversion fructose to furfural on beta zeolite *via* selective carbon-carbon bond cleavage

Yueqing Wang[a,b], Xiaohai Yang[a,b], Hongyan Zheng[d], Xianqing Li[c], Yulei Zhu[a,c,*], Yongwang Li[a,c]

[a] State Key Laboratory of Coal Conversion, Institute of Coal Chemistry, Chinese Academy of Sciences, Taiyuan, 030001, PR China
[b] University of Chinese Academy of Sciences, Beijing, 100049, PR China
[c] Synfuels China Co. Ltd., Beijing, PR China
[d] Department of Chemistry and Chemical Engineering, Taiyuan Institute of Technology, Taiyuan 030008, PR China

ARTICLE INFO

Keywords:
Fructose
Furfural
Beta zeolite
Mechanism
In situ NMR

ABSTRACT

The mechanism for the formation of furfural by dehydration of D-fructose *via* selective carbon-carbon (C—C) bond cleavage was investigated over beta zeolite (Hβ). Several different pore size zeolites were employed to determine the shape selectivity of fructose isomers. Zeolitic pore sizes that smaller than the kinetic diameter of cyclic fructose also produced yield furfural (~22.5%), while the high yield (66.0%) of hydroxymethylfurfural (HMF) can be achieved over large pore zeolite (USY zeolite), which could accommodate the cyclic fructose. These results indicated that the furfural formation likely began with acyclic fructose. *In situ* ^{13}C NMR and GC—MS studies, using labeled ^{13}C-1-fructose as substrate, suggested that the conversion of fructose to furfural involved with splitting of the C5-C6 bond. Furthermore, the C1 compound from the cleavage of C—C bond was identified as formaldehyde, inferring that the selective scission of C—C bond was ascribe to the retro-aldol reaction. Interestingly, *in situ* NMR studies implied that the acyclic fructose mainly derived from pyranose forms. In addition, compared with glucose, fructose directly converted to furfural at the higher yield and reaction rate.

1. Introduction

Research on new and renewable resource have been stimulated by rising demand on fuels and chemicals due to global population growth [1]. As a non-fossil carbon energy resource, lignocellulosic biomass is promising because of its renewability, abundance and wide distribution in nature, and could have minimal environmental impact if it is properly processed [2]. Both hydroxymethylfurfural (HMF) and furfural, as the bridge between lignocellulosic biomass and high add-value fine chemicals, have received renewed attention for production of biofuels and biochemicals [3]. Among the products that can be obtained from cellulose and hemicellulose, furfural is particularly promising, because it can replace petroleum-based raw materials for the production of resins, lubricants, adhesives and plastics [4]. Furfural is also a natural precursor for the production of some valuable furan-based chemicals, such as furfuryl alcohol, tetrahydrofurfuryl alcohol [5], tetrahydrofuran, 2-methylfuran and methyltetrahydrofuran [6]. Nevertheless, HMF is mainly derived from six-carbon sugar or cellulose *via* dehydration and hydrolysis, and its volume is low due to the difficulties in cost-effective production [7]. In contrast, the first commercial production of furfural was started by Quaker Oats in 1921 [5]. Currently, the global demand for furfural is about 300,000–700,000 tons annually. About 70% of furfural is used for the production of furfuryl alcohol, and this demand is expected to rise [8]. Typically, furfural is the natural dehydration product of xylose or arabinose. Although favorable yield of furfural can be achieved in homogeneous catalytic system [9], heterogeneous catalysts has gained increasing attention in order to fully comply with the targets of green chemistry and sustainable production [10–15]. A large variety of heterogeneous catalysts with acidic character including zeolites [11], sulfonated resin [16], heteropolyacid [17] and metal oxide [18], have been studied, and one of the most commonly studied solid acids is zeolites. Currently, furfural was mainly produced from pentose and pentosan. However, it is still a great challenge to obtain furfural directly from hexose. Despite furfural could be produced from hexose under pyrolysis and hydrothermal conditions, the yield of furfural was less than 10–22 % [19–22]. The key development in this area was made by Gürbüz and co-worker, by introducing mordenite and beta zeolite as effective material for the direct conversion of fructose (*a ketohexoses containing six carbon atoms*) to furfural [10]. In addition, previous work [23] from our group also revealed that the high yield (38.5%) of furfural was achieved successfully from cellulose catalyzed by Hβ zeolite. Zeolite has the advantage of shape

* Corresponding author at: State Key Laboratory of Coal Conversion, Institute of Coal Chemistry, Chinese Academy of Sciences, Taiyuan, 030001, PR China.
E-mail address: zhuyulei@sxicc.ac.cn (Y. Zhu).

https://doi.org/10.1016/j.mcat.2018.11.022
Received 12 October 2018; Received in revised form 26 November 2018; Accepted 30 November 2018

selectivity, and makes it possibility to control the pore size and to obtain the optimal structure for intended end use. The unique pore structure of Hβ favors the special selectivity of furfural formation from fructose. It is worthy note that the cellulose is the largest fraction (40-50%) of lignocellulosic biomass, secondly, the proportion of hemicellulose is about 2530% [5]. However, the single production of furfural product from lignocellulose residues would be wasteful, inefficient and uneconomic, because pentosans only contribute a portion of total composition of lignocellulose. Especially, industrial production of furfural from agricultural waste often leaves behind a solid residue containing the amorphous cellulose and lignin [8]. Converting hexose into furfural over Hβ provides a new pathway for the production of valuable chemicals from excessive cellulose and its derived monosaccharides, instead of burning the solid residues in furfural manufacture plant.

However, the precise cleavage of special C−C bond for the production of furfural is a challenging task because there are five C−C bonds with similar bond dissociation enthalpy in fructose molecule. Fructose was the natural precursor for production of C3 polyols or organic acid by retro-aldol reaction, and makes it more difficult for the selective production of furfural by splitting special C−C bond [24,25]. Currently, a variety of catalysts and processes have been studied and developed to convert hexose (fructose and glucose) to organic acid (levulinic acid, lactic acid) and polyols (ethylene, propylene glycol) through catalyzed cleavage of C−C bond, which were nicely summarized and compared in a recent review [26]. A small amount of furfural can be achieved from hexose under the thermal supercritical water without catalysts [22]. It is difficult to perform the special C−C bond scission reaction *via* chemocatalysis at mild condition. However, due to the unique three-dimensional intersecting channels with pore openings size of 6.6 × 6.7 Å and appropriate acid density [27], Hβ zeolite was proved as the promising material for the production of furfural from fructose through selective activation of special C−C bond at mild reaction conditions (140–170 °C). Fundamentally, it is of particular interest to understand how the precise scission of the special C−C bond can be achieved by Hβ zeolite catalyzed. While the mechanisms of fructose transformation to HMF *via* heterogeneous and homogeneous acid catalysts have recently been elucidated, understanding of the furfural formation from fructose in Hβ zeolite is still limited. The formation of furfural from fructose over Hβ zeolite is the complex multistep process with many possible side reactions, which not only associated with the activation of C−O bonds but also the selective cleavage of special C−C bond. It is known that the breaking of C−C bond is the major reaction in petroleum refining processes, and the carbocation mechanism was widely accepted pathway for catalytic cracking and hydrocracking of heavier hydrocarbons [28]. However, the selective cleavage of C−C bond in fructose, containing multiply hydroxyl and carbonyl group, may proceed through different mechanisms. Two possible schemes have been proposed for the formation of furfural during the production of HMF from hexose. One possible pathway is that the fructose was dehydrated to HMF, followed by the elimination of -CH_2O group to generate furfural, based on the observation of 5-hydroxymethylfurfural in pyrolysis process under 350 °C and 500 °C respectively [29]. As a by-product in production process of HMF, another widely accepted explanation is that the formation of furfural was mainly ascribed to the retro-aldol condensation reaction, a familiar process in carbohydrate chemistry. However, the cleavage position of fructose was different depending upon various mechanisms and intermediates. One possible case is that the fructose was firstly converted into 3-keto fructose *via* proton-coupled hydride shift in the presence of Lewis acid sites, then the retro-aldol condensation reaction was performed between C1 and C2 position, in which the pentose was produced with eliminating formaldehyde and the pentose can be transformed to furfural by further dehydration (as shown in ESI†, Scheme S1, route a) [30]. The second case involves enediol intermediate. The five carbon intermediate for production of furfural derived from the different cleavage position of C−C bond. For example, the splitting position was located between C1 and C2 depending on 2,3-enediol, which derived from thermally uncatalyzed process in supercritical water for fructose conversion [19] (as shown in ESI†, Scheme S1, route b). Whereas, the breaking of C−C bond occurred between C5 and C6 from 1,2-enediol intermediate may explaining the limited formation of furfural over mordenite [31] (as shown in ESI†, Scheme S1, route c).

Despite several assumptions have been proposed, it is not yet well understood if furfural is formed directly from the fructose or HMF, or *via* another intermediate over Hβ zeolite so far. In present paper, we studied the mechanism of the conversion fructose to furfural over Hβ zeolite on the basis of several aspects: (i) identifying fructose isomer for furfural formation with zeolitic shape selectivity, (ii) identifying the position of C−C bond scission using isotopic labeling method and (iii) *in situ* monitoring the isomers for formation of furfural. In order to understand how the C−C bond scission in bio-based fructose occurs over Hβ zeolite, *in situ* ^{13}C NMR was employed to trace the isotopic carbon of fructose mapped into which carbon of furfural. It was found that the retro-aldol process was easily catalyzed by Hβ zeolite to produce the C5 + C1 products. Therefore, accurate understanding of mechanism of furfural formation *via* selective cleavage of C−C bond on Hβ zeolite at molecular level could help the design of high selective catalyst to enhance furfural yield.

2. Experimental section

2.1. Materials and instruments

Fructose (analytical grade, 99.5%), glucose (analytical grade, > 99.0%) 5-hydroxymethylfurfural (HMF, > 99.0%), furfural (≥ 99.5%) and γ-butyrolactone (GBL, chromatographic grade, 99.9%) were obtained from Shanghai Aladdin Co., Ltd., (^{13}C-1)-fructose (99 atom %) was purchased from Cambridge Isotope Laboratories (CIL). D_2O (99.8 atom %) was also obtained from CIL, and zeolites from Nankai University Catalyst Co., Ltd.. All reagents were used as received without further purification in this work.

Liquid phase ^{13}C nuclear magnetic resonance (NMR) spectra were obtained by using Bruker AVANCE 400 spectrometer equipped with a variable temperature probe. The chemical shifts were referenced to an external standard of D_6-dioxane. The ^{13}C spectrum was obtained at 100 MHz, and the relaxation delay was 10 s.

2.2. Fructose dehydration and analysis

All experiments were carried out in a batch reactor with magnetic stirrer. Typically, 1.7 wt% initial materials and a certain volume solvent were added into stainless vessel, followed by the addition of the catalyst Hβ (0.3 wt %). Before each run the vessel was sealed and flushed with N_2 to exclude air for three times. After the reaction is completed, the vessel was immediately immerged in ice bath. The reaction products were centrifuged for 5 min and then filtrated to obtain a clear solution. The samples were analyzed by GC (Agilent 7890) using an instrument equipped with an AB-INNOWAX capillary column (30 m × 0.32 mm × 0.5 μm). Standard solutions were used to obtain the calibration curves to calculate the concentrations of compounds by the external standard method. The content of sugar was determined by HPLC (Agilent 1260) with a Shodex SH-1821 capillary column (300 mm × 8 mm × 0.6 mm). Standard solutions were used to obtain the calibration curves to calculate the concentrations of the compounds by the external standard method.

The conversion of substrate and the yield of products were quantified according to the following equations:

$$Conversion\ (mole\ \%) = \frac{mole\ of\ sugar\ (inlet) - mole\ of\ sugar\ (outlet)}{mole\ of\ sugar\ (inlet)} \times 100\%$$

$$Yield\ (mole\ \%) = \frac{mole\ of\ one\ product\ produced}{mole\ of\ theoretical\ product\ value} \times 100\%$$

Gas chromatography-mass spectrometry (GC–MS) was then used to identify the labeled products. The sample was analyzed by an Agilent G2579 A series GC system connected to an Agilent G1530 M quaternary pole mass detector, using electrospray ionization (EI) 70 eV in the positive mode. A 30 m × 0.32 mm × 0.5 μm, AB-INNOWAX column was used, and 1 ml/min helium was used as carrier gas. Products were identified by comparison of their mass spectra and retention times with corresponding standard spectra in NIST libraries.

2.3. Procedure for in situ NMR studies

10 mg labeled (^{13}C-1)-fructose and 4 mg Hβ zeolite were added in 0.5 ml γ-butyrolactone (GBL) with 5 wt % water. The mixture solution was sonicated after it was added into the coaxial NMR tube. The NMR tube was heated to 170 °C with sand bath. The reaction was immediately quenched by immersing the NMR tube in an ice-bath, and the ^{13}C (rd = 10 s, NS = 256) NMR spectra was recorded using condition identical to the t = 0 min spectrum. Acetone was added to the coaxial NMR tube as external standard for *in situ* quantitative analysis of fructose isomers.

2.4. NMR study of D-fructose tautomer distribution

A low concentration of 0.027 M (mole/L) was adopted in order to avoid possible contribution of solute-solute interaction, and labeled (^{13}C-1)-D-fructose was fully dissolved in the mixture solvent (GBL/H_2O) in the course of ^{13}C NMR measurements. When GBL contented 5 wt % H_2O was used as solvent, appropriate D_2O was added in coaxial NMR tube by using the deuterium resonance of D_2O as the lock signal. The composition of fructose tautomer was analyzed by ^{13}C NMR (The pulse sequence was zgpg 30, the relaxation delay was 10 s, 128 scans.) until to reach the equilibrium.

2.5. Catalysts characterization

FTIR spectroscopy was employed to distinguish the acyclic and cyclic form of fructose. The FTIR spectra were recorded on a Bruker VERTX 70 FTIR spectrophotometer, equipped with deuterium triglycine sulfate (DTGS) detector. The power samples were mixed with KBr and pressed to translucent disks. The spectra were recorded between 4000 cm^{-1} and 400 cm^{-1}.

The X-ray diffraction (XRD) patterns were recorded on a BrukerAxs D2 diffractometer with Cu Kα radiation (λ = 1.54 Å) at 30 kV and 10 mA with scanning angles (2θ) in the range of 5°-60°.

3. Results and discussion

3.1. Furfural formation over Hβ zeolite

Initially, furfural was produced from fructose and 5-hydroxymethylfurfural (HMF) over Hβ zeolite. The furfural yields for different temperature (Entry 1–7) were shown in Table 1. The yield of furfural was increased with increasing of reaction temperature. Although favourable yield of furfural was obtained at low temperature, the ratio of yield between furfural and HMF is lower, compared with those obtained at elevated temperature (Entry 1–2). In addition, furfural was more stable than HMF at elevated temperature (160–180 °C). Compared with low temperature, the degradation of fructose was partly suppressed at high temperature because most fructose was converted to furfural. Although high yield furfural could be obtained from fructose over Hβ zeolite, the formation mechanism is not yet clear. In order to further investigate the mechanism, the production of furfural was studied *via* experiments under optimal condition using HMF as initial material.

Table 1
The formation of furfural from fructose in different temperature[a].

Entry	Temp. (°C)	Conv.(%)	Yield (%)			
			Furfural	HMF	Glucose	others
1	100	62.9	11.0	9.2	/	4.8
2	120	91.2	33.8	25.2	6.4	4.9
3	140	99.9	47.9	29.4	3.4	12.3
4	150	99.9	49.8	24.3	1.7	13.5
5	160	99.9	50.7	23.5	1.4	17.6
6	170	99.9	51.8	19.3	1.7	19.9
7	180	99.9	50.7	16.8	0.4	18.4
8[b]	170	5.6	/	/	/	3.0

[a] All experiments were carried out in a monophasic system, containing either 1.7 wt % feed, 0.3 wt% Hβ and 5 wt % H_2O in GBL were used in all cases, each runs were hold for 50min. GBL = γ-butyrolactone; others: formic acid, levulinic acid.
[b] Start from HMF under the same condition.

Since no obvious furfural was formed from HMF, it could be concluded that both furfuran and HMF were directly derived from fructose *via* competitive reaction roots rather than sequential reaction (Entry 8). Glucose as another by-product could be ascribed to the isomerization of fructose in the presence of Lewis acid sites.

3.2. The fructose isomers analysis for furfural formation

The presence of a variety of isomers makes it difficult to analyze the mechanism of fructose conversion. In order to elucidate the mechanism for furfural formation, it is important to understand how the fructose isomers reach equilibrium under room temperature. In solution, fructose adopts five structural conformations: β-pyranose, β-furanose, α-furanose, α-pyranose and linear keto form as shown in Scheme 1, the isomers could be transformed between each other *via* linear keto form. To help understand the complicated structures of fructose, an abbreviated notation are adopted for the fructose isomers.

Furthermore, the furanose (five-membered ring) and pyranose (six-membered ring) form can be denoted as *fur* and *pyr*. By this, for example, the β-furanose of fructose is denoted as *β-fur*. Importantly, the tautomer distribution have a significant influence on product selectivity, the pyranose forms is prone to produce humins, while furanose forms is more likely to produce HMF by eliminating three water molecules [32–34]. Now we discuss the pathway of furfural formation over Hβ zeolite by focusing not only on the products but also on the isomers. Despite the isomers could be distinguished by ^{13}C NMR spectroscopy, the low isotopic ratio of ^{13}C as compared to ^{12}C make the detection of minor isomers are time consuming.

Additionally, due to the ratio of isomers is changing as time goes on, the ^{13}C NMR spectroscopy can be combined with a site selective labeling technique that enables us to dynamically identify competing isomers. To this end, the high-resolution ^{13}C NMR measurement carried out as function of time by taking advantage of site selectively labeled ^{13}C-1-fructose at room temperature. As previous shown, the open chain and cyclic forms of fructose are all observed in γ-butyrolactone (GBL) containing 5 wt % water: *β-pyr* (65.11 ppm), *β-fur* (63.89 ppm), *α-fur* (64.11 ppm), *α-pyr* (64.70 ppm) and keto form (66.85 ppm), where the parenthesized numbers are the ^{13}C chemical shifts of C1 carbon atom of interest (as shown in ESI†, Figure S1). According to the integrated peak intensities, the proportions of isomer fructose are determined at different times up to equilibrium. The relevant results have been shown in Fig. 1, the following tendencies are observed: (i) the six-membered fructose of type *β-pyr* decrease with time, and correspondingly, the other isomeric forms increase, and (ii) the *β-pyr* form was the major form at equilibrium status, following the five-membered fructose of type *β-fur*. These transformation tendencies could be accelerated with

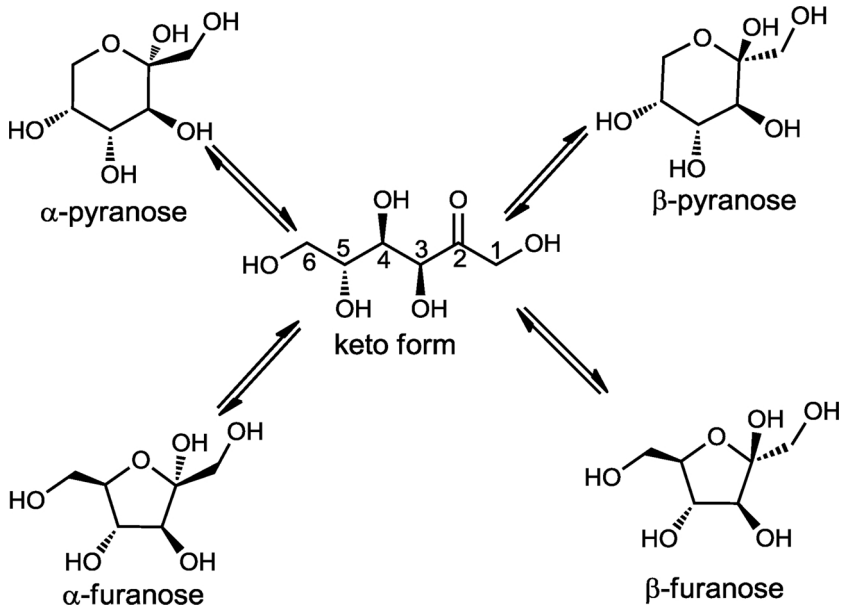

Scheme 1. The structure and isomerization of fructose isomers.

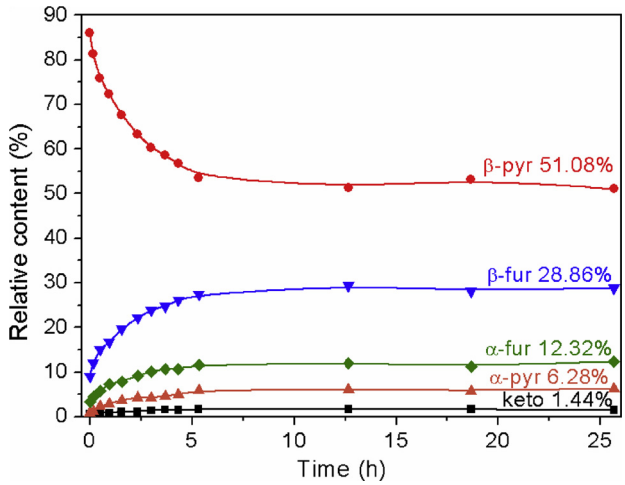

Fig. 1. The isomerization of fructose with time; β-pyr = β-pyranose, β-fur = β-furanose, α-fur = α-furanose, α-pyr = α-pyranose, keto = linear fructose.

increasing of temperature, even other isomers such as *β-fur* could predominate at high temperature [35]. In order to further investigate the relationship between isomers distribution and furfural formation, some experiments were designed as follows. According the equilibrium rule mentioned above, a certain amount of fructose solution containing 1.7 wt % (maximal dissolution in GBL containing 5 wt % H_2O) was equilibrated for 20 h at room temperature. Once the reaction temperature reached the set value (170 °C), the fructose solution was immediately added into the reactor, and hold for 50 min. Meanwhile, another experiment was carried out under the same condition for comparison using solid fructose as initial material. The distribution rule of fructose isomers allows us to assume that the pre-equilibrium procedure make more *β-fur* form to participate for furfural formation, while the reaction directly using solid fructose could be regarded as the major *β-pyr* form.

However, as shown in Table 2, regardless of the isomers was equilibrated or not, both the yield of furfural and HMF was no obvious distinction. These results indicated that the yield of furfural was not limited to the amount of cyclic fructose isomers. If equilibrium rate between five isomers was slower than the dehydration, the distribution of products should be depended on the ratio of pyranose and furanose

Table 2
The influence of isomers for furfural formation[a].

			Yield (%)	
Entry	Feedstock	Conv.(%)	Furfural	HMF
1	Equilibrated solution	99.9	48.6	14.5
2	Solid fructose	99.9	49.0	15.5

[a] All experiments were carried out in GBL containing 5 wt % water at 170 °C. Once the temperature was reached set value, the feeds were immediately added in.

forms, but the experiments exhibit the adverse results. This suggested to us that the furfural may be derived from the same precursor either pyranose or furanose was predominate. According to present analysis and previous reports, the mostly possible pathway is that the conversion of fructose into furfural begins with keto form, while the equilibrium rate between furanose, pyranose and keto forms was sufficiently faster to replenish the keto form than the dehydration and cleavage reaction of C—C bond kinetics. However, the evidence is yet insufficient with respect to the isomers distribution investigation. To this end, the further investigation should be carried out in view of zeolitic shape selectivity.

3.3. The shape selectivity to tautomer

The shape selectivity is classically defined as being caused by the effects of mass transport and transition state [36,37]. Therefore, the unique pore structure of zeolitic materials endows them with special selectivity for reactants or transition state at molecular level. Specific pore window size of zeolites limits certain reactant molecules, so shape selectivity restricts certain reactant and influences the course of reaction. Zeolites with medium pore size (ZSM-22, ZSM-5, MCM-22), large pore zeolites (beta) and cavity zeolite (USY) are employed to get insight into the shape selectivity on the fructose conversion pathway and mechanism. The kinetic diameter for the products and reactant was estimated from literature value to determine whether the reactions occur inside the pores or on the external surface [27]. The kinetic diameters of cyclic fructose, furfural and HMF were estimated as 8.6 Å, 5.5 Å and 6.2 Å, respectively [27,38]. Additionally, the pore window sizes of zeolites calculated with atomic radii are smaller than those adjusted with Norman radii. The Norman radii is related to the diffusion of

Table 3
The shape selectivity of zeolitic catalysts[a].

Entry	Zeolite[b]	Pore size (Å)	Maximal pore size[c]	Conv. (%)[d]	Yield (%)		
					Furfural	HMF	Others
1	ZSM-22	4.5 × 5.2	5.9	96.6	22.5	33.4	4.0
2	ZSM-5	5.1 × 5.5 5.3 × 5.6	6.2 and 6.3	96.4	21.2	36.3	5.5
3	MCM-22	4.0 × 5.5 4.1 × 5.1	6.2 and 5.8	99.9	22.5	33.1	6.5
4	Beta	6.6 × 6.7 5.6 × 5.6	7.4 and 6.3	99.9	51.8	19.3	19.9
5	USY	7.4 × 7.4	8.1	94.2	10.3	66.0	1.7
6	A-15	/	/	99.9	trace	37.8	22.8
7	γ-Al_2O_3 + A-15	/	/	82.3	trace	38.6	6.9

[a] Pore window size of zeolites used in this study from the international zeolite association [39].
[b] The XRD patterns of zeolites used in present work have been shown in ESI†, Figure S2.
[c] Adjusted by Norman radii.
[d] All experiments were carried out in GBL containing 5 wt % water, 1.7 wt % fructose and 0.3 wt % catalysts. Each runs was hold for 50 min at 170 °C. Others: formic acid, levulinic acid; A-15: Amberlyst 15.

molecules whose diameter is larger than the size of crystallographic pore [27]. Therefore, the pore sizes adjusted by Norman radii are used to compare the zeolite pore sizes with kinetic diameter of molecules in this work. The results have been listed in Table 3, and medium pore zeolites produced favorable yields of furfural (Entry 1–3).

Jungho Jae and co-workers pointed out that the cyclic glucose could be excluded out pore of ZSM-5 [27], as such the cyclic fructose is significantly larger than the maximum pore size of ZSM-22, ZSM-5 and MCM-22; it would not be expected to diffuse into the zeolite pore. Therefore, the favorable yield of furfural from medium pore zeolites indicated that the formation of furfural is likely derived from linear fructose, which has the smaller cross section diameter and flexible to diffuse through the pores of zeolites [38]. The yield of HMF was slight higher than furfural from medium pore zeolites, indicating that the more cyclic fructose molecule were converted on the external surface of zeolite than the inside of pore due to increased diffusion resistance. These results were further confirmed by using imporous Amberlyst 15 + Al_2O_3 catalyst (Entry 7), from which favourable yield HMF was achieved. Importantly, the highest yield of furfural was obtained over the large pore size of zeolite (beta) without cavities, while the USY zeolite containing large pore and 1.3 nm cavities results in high yield of HMF. However, some previous reports [40–42] suggested that cyclic fructose could diffuse in the large pore of Hβ. In order to further investigate the mechanism of furfural formation, the FTIR characterization was employed, because carbonyl vibration peak of acyclic fructose was observed in carbonyl region but this peak was absence in ring structure fructose. Considering that carbonyl peak of γ-butyrolactone is also located in the carbonyl region, the dioxane was chosen as replace solvent. As shown in Fig. 2A, the vibration peak at 1768 cm^{-1} was observed, assigned to the carbonyl group of acyclic fructose, in the fructose/Hβ system. Moreover, the very weak vibration peak at 870 cm^{-1} and 930 cm^{-1} were also observed, which could be assigned to ring structure fructose [43,44]. In contrast, as shown in the Fig. 2B, only bands at 870 cm^{-1} and 891 cm^{-1} were observed with disappearing of peak at 1768 cm^{-1} in the fructose/USY system.

These results indicated that the cyclic fructose could actually diffuse in the pores of Hβ zeolite, but fraction of acyclic fructose was enriched in the channel of Hβ. Interestingly, furfural was the major product with acyclic fructose, while the HMF was dominant without open-ring fructose on cavities zeolite (USY). That is, the distinction of channels between USY and Hβ played an important role in the selectivity of products. Compared with Hβ, the cavities endow USY enough space to accommodate the cyclic fructose, which feasible to produce HMF. Whereas the intersecting straightly three-dimensional channels of Hβ make acyclic tautomer to be enriched in it, and thus the furfural was dominant product. On the basis of these experimental results from FTIR characterizations, it is concluded that the high yield of furfural was achieved mainly due to the shape selectivity of Hβ to tautomer, and the acyclic fructose favors the formation of furfural within the Hβ pores. In addition, only trace furfural was detected over γ-Al_2O_3 and Amberlyst-15 catalyst, indicating that the appropriate pore size other than the properties of Brønsted and Lewis acid play the key role for the formation of furfural (Entry 7). However, it is not clear which C—C bond is split over Hβ zeolite, and the selective isotopic labeling technique was used to address this problem. Further ^{13}C NMR and GC—MS analysis are carried out using labeled fructose in followed section.

3.4. *In situ* ^{13}C NMR analysis for furfural formation

The first carbon (C-1) labeled fructose was examined to determine which carbon atom (C-1 or C-6) is converted to the carbonyl carbon in furfural. Fig. 3 shows the *in situ* ^{13}C NMR spectrums as a function of reaction time for the conversion fructose to furfural with Hβ in GBL containing 5 wt % H_2O at 170 °C. The NMR peaks (64.05, 64.1, 64.9, 65.3 and 66.8 ppm) of C-1 carbons were identified as the five main anomeric forms of fructose in the baseline spectrum taken at t = 0 min in Fig. 3b, or the *β-fur*, *α-fur*, *α-pyr*, *β-pyr* and acyclic forms as reported by Thomas Barclay [45].

Although weak isotopic NMR peaks were visible in the carbonyl region, which was not the GBL ester group (178.6 ppm), the fructose resonance peaks was dominate on the ^{13}C NMR spectrum recorded at t = 5 min (Fig. 3b and c). Compared with other characteristic peaks of furfural and HMF, which are too weak to be visible in the Fig. 3a, the overlapping peaks at 178.5 and 178.2 ppm corresponding to the aldehyde moiety of furfural and HMF respectively in carbonyl region is greatly enhanced due to ^{13}C enrichment. Moreover, the intensity of both peaks at 178.2 and 178.5 ppm was increased and the intensity of peaks assigned to the fructose correspondingly decreased with increasing of time. The peaks ascribed to cyclic intimidate, which is proposed as a precursor for the formation of HMF [35], was not observed in our experiments. As the reaction time prolongs to 100 min, the NMR peaks in the carbonyl region become apparent and the peaks in anomeric carbon region are invisible except peaks at 64.8 ppm (anomeric carbon of linear form). This result manifested that the aldehyde carbon of furfural may be originated from the C1 of fructose. However, it is difficult to identify the chemical shift of furfural and HMF, because of the chemical shift was strong affected by the chemical environment such as polarity or solvent composition. In our experiments, the chemical shift of ester group ascribed to GBL was shifted 0.6 ppm to low-field due to the formation of water in the process of dehydration. The chemical shift of furfural and HMF was also suffered from the same effect. Additionally, the resonance peaks could be significant enhanced by little isotopic products. Therefore, the further experiments should be carried out to distinguish the resonance peak of furfural. Both furfural and HMF at a ratio of 1:1 by weight were added in the mixture of GBL and 5 wt % water. The NMR spectrum was

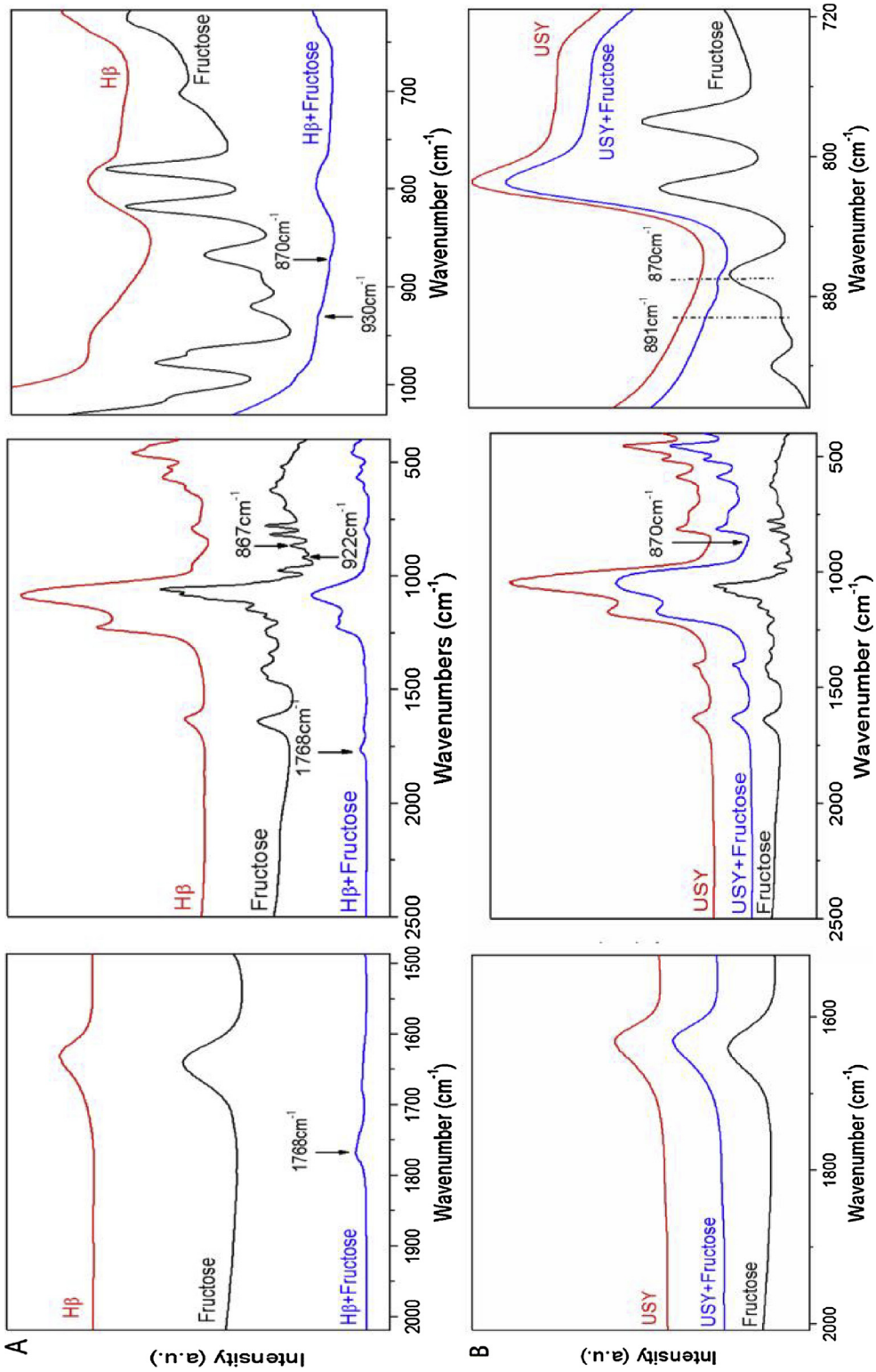

Fig. 2. The FTIR spectra of A) fructose + Hβ; B) fructose + USY.

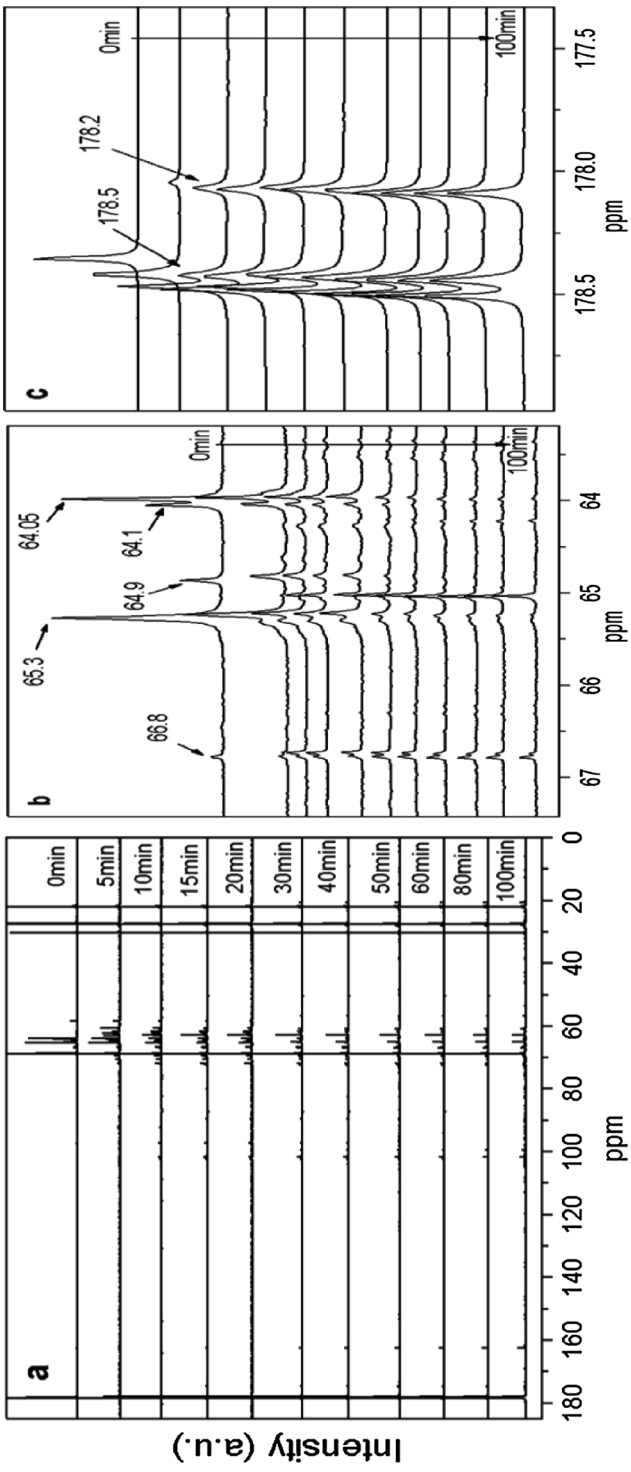

Fig. 3. *In situ* ^{13}C NMR spectra as a function of time for (^{13}C-1)-fructose conversion catalyzed by Hβ at 170 °C, a) 13C NMR spectra, b) enlarged spectra between 64–67 ppm, c) enlarged spectra between 177–180 ppm.

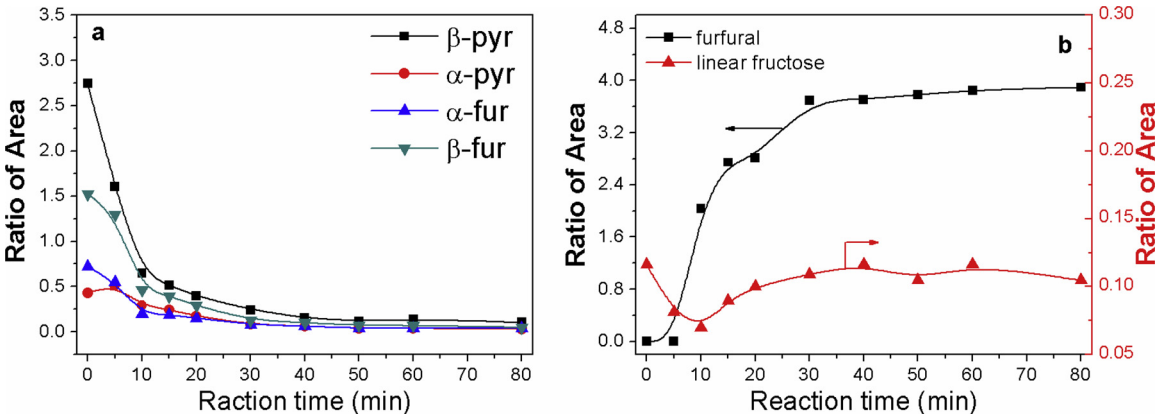

Fig. 4. The content of fructose isomers as a function of time, Y value represent the ratio of samples and external standard peak area, *pyr* = pyranose, *fur* = furanose.

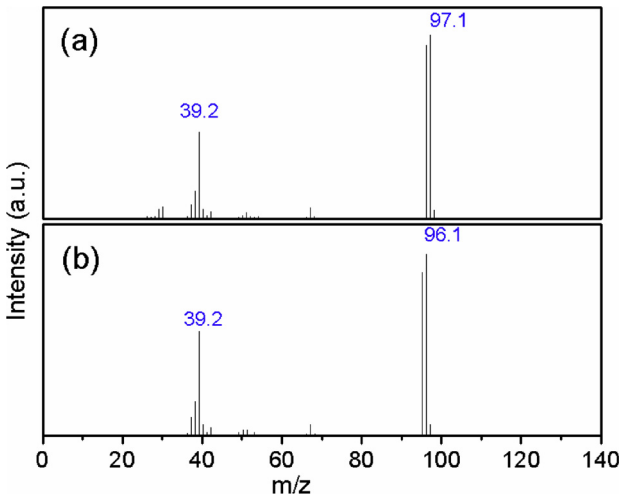

Fig. 5. The mass spectrum: (a) ^{13}C-1-fructose and (b) fructose dehydration catalyzed by Hβ.

recorded, after furfural was added at ratio 2:1 and recorded again under the same condition. Compared the ratio of peak area before and after the addition of furfural, the intensity of peak at 178.5 ppm was obviously increased, and the peaks at 178.5 ppm and 178.2 ppm could be distinguished. The former was assigned to aldehyde group of furfural, and the peak at 178.2 ppm should be ascribed to carbonyl carbon atom of HMF (as shown in ESI†, Figure S3). Therefore, it is clarified that the aldehyde moiety carbon atom was derived from C1 of fructose, and the conversion of fructose to furfural involves splitting of C5-C6 bond in linear fructose inside pore of Hβ.

Additionally, the distribution of five isomers was dynamically monitored with increasing of reaction time, based on the integration of anomeric carbon NMR peaks. The distribution of isomers was recorded during initial reaction period when the temperature was reached to set value. A certain amount of unlabeled acetone was added as external standard for quantitative analysis, and the group $-CH_3$ (30.3 ppm) was chosen as standard. As shown in Fig. 4a and b, the contents of acyclic fructose gradually decline and furfural increased during the initial period, then content of acyclic fructose gradually increased and other cyclic forms decreased. Moreover, as Fig. 4b shown, the content of furfural was increased with increasing of acyclic fructose, and the equilibrium was achieved at 40 min when the content of furfural and linear fructose was almost unchanged. Blank experiments were carried out under the same condition without catalyst (as shown in ESI†, Figure S4), the equilibrium of isomers was reached within 10 min and maintained until 50 min. However, this process was slow with Hβ (Fig. 4a), the decreasing of furanose forms might be caused by the formation of HMF and partial acyclic fructose. As proposed in the previous reports [45,46], the conversion between each isomers of fructose was a reversible equilibrium reaction, and the pyranose forms of fructose rapidly was converted to furanose forms *via* linear keto intermediate. The reverse process occurs in a similar way. In our experiments, the pyranose forms were consumed faster than furanose, indicating that the acyclic fructose was mainly derived from pyranose forms. Compared with blank experiments where furanose forms were dominant without catalyst, the furfural was a major product catalyzed by Hβ. It indicated that the equilibrium has been changed over Hβ, and the cyclic fructose was transformed into acyclic (as shown in Fig. 4a and ESI†, Figure S4). *In situ* observations provide direct evidence that the unique pore structure endows Hβ zeolite with special shape selectivity to facilitate the formation of keto fructose. Based on the analysis above, both the formation of furfural and HMF were proved to start from different isomers, the furfural mainly derived from linear fructose, while the HMF was originated from furanose forms. The unique pore structure of Hβ facilitates the conversion of both cyclic pyranose and furanose forms to acyclic form. This may explain why furfural was the major product.

Moreover, the gas chromatography-mass spectrometry (GC—MS) experiments were performed to further determine either C-1 or C-6 becomes the carbonyl group in furfural during the catalyzed dehydration of fructose over Hβ.

As shown in Fig. 5, the furfural molecule with a MW of 97.1 was observed when using C-1 labeled fructose as initial material, while unlabeled fructose produced an ion of *m/z* 96.1 normal molecular weight. This is consistent with the observation from the NMR studies. This result further confirms that the C-1 of fructose is converted to the aldehyde moiety of furfural. Furthermore, the C1 compound from C—C bond scission was identified as formaldehyde based on the MS spectrum analysis (as seen in ESI†, Figure S5). Based on isotopic ^{13}C NMR, shape selectivity and GC—MS analysis, it could be proposed that the formation of furfural began with acyclic fructose, and the elimination of the C6 moiety in fructose dominated over the elimination of C1 moiety due to the unique pore structure of Hβ. Then, the C5 intermediate was further converted to furfural inside pore of Hβ. Additionally, both the route a and b (as shown in ESI†, Scheme S1) were ruled out by *in situ* isotopic NMR and GC—MS studies. Moreover, the cleavage of C5-C6 bond could be ascribed to the retro-aldol reaction.

3.5. Mechanism of furfural formation

In situ ^{13}C NMR and GC–MS studies using labeled isotope fructose has ruled out the route a and b. Although the route c could explain the experiments results, previous reports [47,48] suggested that it was not feasible to form the initial key intermediate (1,2-enediol) over Hβ, which contained Lewis and Brønsted acid sites. The 1,2-enediol was widely observed during the isomerization between glucose and fructose

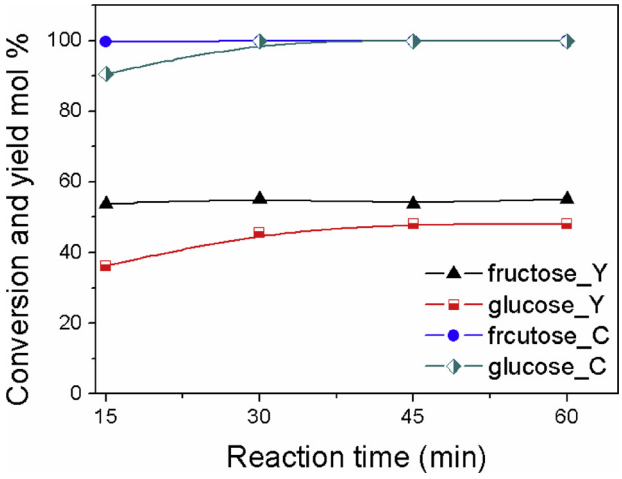

Fig. 6. Furfural yields from glucose and fructose vs reaction time (fructose_Y and glucose_Y are the yield of furfural from fructose and glucose respectively, fructose_C and glucose_C represent conversion.).

under alkaline condition. Moreover, Davide Carnevali and his co-worker developed a gas-phase process for conversion fructose to furfural (~22%) in oxidizing environments. They proposed that the furfural was produced by eliminating formic acid in the first step [49]. However, this possible pathway was also ruled out by our experiments stem from the fact that the C1 compound was identified as formaldehyde by GC–MS. Some studies suggested that glucose could be converted to furfural *via* 3-deoxyglucose intermediate [21,50,51], and glucose (aldose, isomeride of fructose) was detected in our all experiments (Table 1). Therefore, the fructose could be transformed into furfural through isomerization, dehydration and retro-aldol reactions. In order to further confirm this proposal, experiments were carried out using glucose and fructose as substrate, respectively, at 170 °C for different time.

As shown in Fig. 6, the yield of furfural obtained from glucose is lower than those from fructose, and maximal yield of furfural occurred at 15 min for fructose when it was converted completely, but the maximal yield for glucose appeared after more than 30 min and the conversion was still not complete. These results apparently implied that the fructose did not undergo 3-deoxyglucose pathway. Therefore, fructose and glucose were converted to furfural *via* different pathway (as shown in ESI†, Table S1). Our previous studies [52] point out the octahedrally framework aluminum may function as an important active sites for splitting C—C bond. The formation of furfural was possible ascribe to the synergistic effect between acid sites (Lewis and Brønsted acid sites) and octahedrally framework aluminum. The selective scission of C—C bond most likely occurred *via* the retro-aldol reaction. The retro-aldol reaction is common in the glycolysis catalyzed by aldolase A enzymes, in which the fructose-1,6-bisphosphate was cleaved into dihydroxyacetone and glyceraldehyde-3-phosphate. The same reaction was realized over chemical catalyst with unique pore structure and active sites in this work. Furthermore, the effects of acid sites were also investigated using ion-exchanged method. Tervalent ion such as Fe^{3+} was selected to tune the acidity of Hβ, and the high silicon (SiO_2/Al_2O_3 = 40) Hβ was also employed to evaluated the effect of acid sites. As shown in Table 4, the density of Lewis acid sites was significantly decline with introducing of Fe^{3+} (as shown in ESI, method section). Consequently, the yield of furfural decline from 50.7% to 27.5% with decrease of Lewis acid sites, while the small change of Brønsted acid has slight influence on the yield of furfural (Entry 2).

These results indicated that the Lewis acid sites may function as active sites for scission of C—C bond, while the dehydration reaction was performed on Brønsted acid sites. Therefore, it was concluded that fructose was converted to furfural *via* the opening of ring of pyranose fructose, followed by the β-elimination between OH at C3 and H at C4, as shown in Scheme 2 below. According to the retro-aldol rule or double bond rule, the double bond between C3-C4 facilitates the splitting of C5-C6 bond. Additionally, the enol may be the more preponderant form than its keto because of the electron-withdrawing properties of carbonyl at C2.

The C5 intermediate was formed by eliminating the C6 as formaldehyde, then it was converted to five-membered ring by hemiacetal reaction between OH at C5 and C = O at C2. Finally, the furfural was produced by eliminating last two water molecules. Moreover, the formation of furfural *via* HMF has been ruled out by using HMF as substrate.

4. Conclusion

The mechanism of fructose conversion to furfural has been investigated using *in situ* NMR with isotope ^{13}C labeling. Hβ zeolite exhibits unique shape selectivity for fructose isomers, and the acyclic isomer was likely an effective precursor for furfural formation. The *in situ* ^{13}C NMR studies point out that fructose was converted to furfural by splitting of C5-C6 bond. *In situ* monitoring of the acyclic and other cyclic isomers was using ^{13}C NMR indicated that the acyclic isomer was mainly derived from *β-pyr* forms and partially from *fur* isomers, and more furfural was produced with increasing of acyclic fructose. Moreover, the C1 compound, which was removed from terminal (C6) of fructose, was identified as formaldehyde by GC—MS. These results implied that the selective scission of C—C bond could be ascribed to the retro-aldol reaction. Furthermore, fructose was different from glucose in mechanism of furfural formation, and the fructose undergoes a pathway with high reaction rate and yield. Based our investigation, furfural is mainly derived on active sites from inside pores, and acyclic fructose was mainly transformed from *pyr* isomer. Therefore, tuning the external/internal active sites will contribute to the selectivity of furfural. However, the formation of HMF was inevitable because of the presence of furanose fructose.

Acknowledgements

The authors gratefully thank the financial supports of the National

Table 4
The effect of acid sites[a].

Entry	Catal.	SiO_2/Al_2O_3[b]	Conv.(%)	Yield (%)			Acid density (mmol/g)[c]		
				Furfural	HMF	Others	Brønsted	Lewis	B/L
1	Hβ	25	99.9	50.7	23.5	17.6	0.28	0.17	1.65
2	Hβ	40	99.9	45.6	22.8	15.9	0.18	0.16	1.12
3[d]	Fe/Hβ	46	99.9	27.5	20.0	7.1	0.14	0.06	2.33

[a] All experiments were performed at 160 °C for 50 min, 1.7 wt% feedstock, 0.3 wt% catalyst, others = formic acid and levulinic acid.
[b] Determined by ICP analysis.
[c] The acid density was determined after desorption at 200 °C.
[d] The Fe/Hβ was derived from Hβ (SiO_2/Al_2O_3 = 25) by ion-exchanger method, the value of Fe/Al is 1.

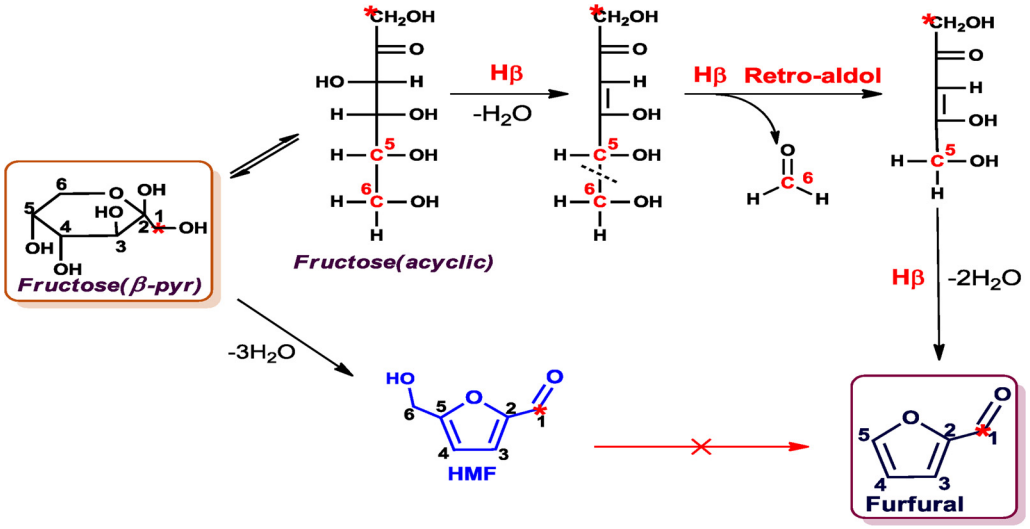

Scheme 2. The possible pathway for formation of furfural.

Natural Science Foundation of China (No. 21875276), Shanxi Science and Technology Innovation Team of Biofuels & Chemicals, Institute of Coal Chemistry, Chinese Academy of Sciences, Taiyuan, P R China. The authors also thank Yingxiong Wang Researcher of Institute of Coal Chemistry for NMR technical assistance.

Appendix A. Supplementary data

Supplementary material related to this article can be found, in the online version, at doi:https://doi.org/10.1016/j.mcat.2018.11.022.

References

[1] J.A. Melero, J. Iglesias, A. Garcia, Energy Environ. Sci. 5 (2012) 7393–7420.
[2] R. Mariscal, P.M. Torres, M. Ojeda, I. Sádaba, M.L. Granados, Energy Environ. Sci. 9 (2016) 1144–1189.
[3] J.J. Bozell, G.R. Petersen, Green Chem. 12 (2010) 539–554.
[4] L.C. Nhien, N.V.D. Long, S. Kim, M. Lee, Biotechnol. Biofuels 10 (2017) 81.
[5] X. Li, P. Jia, T. Wang, ACS Catal. 6 (2016) 7621–7640.
[6] J.P. Lange, E. van der Heide, J. van Buijtenen, R. Price, ChemSusChem 5 (2012) 150–166.
[7] C. Moreaua, M.N. Belgacemb, A. Gandini, Top. Catal. 27 (2004) 11–30.
[8] A.S. Mamman, J.M. Lee, Y.C. Kim, I.T. Hwang, N.J. Park, Y.K. Hwang, J.S. Chang, J.S. Hwang, Biofuels, Bioprod. Bioref. 2 (2008) 438–454.
[9] A.S. Dias, M. Pillinger, A.A. Valente, Appl. Catal. A Gen. 285 (2005) 126–131.
[10] E.I. Gurbuz, J.M. Gallo, D.M. Alonso, S.G. Wettstein, W.Y. Lim, J.A. Dumesic, Angew. Chem. Int. Ed. 52 (2013) 1270–1274.
[11] S. Lima, M. Pillinger, A. Valente, Catal. Commun. 9 (2008) 2144–2148.
[12] C.G. Sancho, I. Sadaba, R.M. Tost, J.M. Robles, J.S. Gonzalez, M.L. Granados, P.M. Torres, ChemSusChem 6 (2013) 635–642.
[13] I.A. Telleria, J. Requies, M.B. Güemez, P.L. Arias, Appl. Catal. B: Environ. 145 (2014) 34–42.
[14] I.A. Telleria, J. Requies, M.B. Güemez, P.L. Arias, Appl. Catal. B: Environ. 115-116 (2012) 169–178.
[15] I. Sádaba, M. Ojeda, R. Mariscal, M.L. Granados, Appl. Catal. B: Environ. 150-151 (2014) 421–431.
[16] E. Lam, E. Majid, A.C. Leung, J.H. Chong, K.A. Mahmoud, J.H. Luong, ChemSusChem 4 (2011) 535–541.
[17] A.S. Dias, S. Lima, M. Pillinger, A.A. Valente, Carbohydr. Res. 341 (2006) 2946–2953.
[18] A. Dias, S. Lima, D. Carriazo, V. Rives, M. Pillinger, A. Valente, J. Catal. 244 (2006) 230–237.
[19] T.M. Aida, Y. Sato, M. Watanabe, K. Tajima, T. Nonaka, H. Hattori, K. Arai, J. Supercrit. Fluids 40 (2007) 381–388.
[20] P.R. Patwardhan, J.A. Satrio, R.C. Brown, B.H. Shanks, J. Anal. Appl. Pyrolysis 86 (2009) 323–330.
[21] F. Jin, H. Enomoto, Energy Environ. Sci. 4 (2011) 382–397.
[22] T.M. Aida, K. Tajima, M. Watanabe, Y. Saito, K. Kuroda, T. Nonaka, H. Hattori, R.L. Smith, K. Arai, J. Supercrit. Fluids 42 (2007) 110–119.
[23] J. Cui, J. Tan, T. Deng, X. Cui, Y. Zhu, Y. Li, Green Chem. 18 (2016) 1619–1624.
[24] M.S. Holm, S. Saravanamurugan, E. Taarning, Science 328 (2010) 602–605.
[25] N. Ji, T. Zhang, M. Zheng, A. Wang, H. Wang, X. Wang, J.G. Chen, Angew. Chem. Int. Ed. 47 (2008) 8510–8513.
[26] W. Deng, Q. Zhang, Y. Wang, J. Energy Chem. 24 (2015) 595–607.
[27] J. Jae, G.A. Tompsett, A.J. Foster, K.D. Hammond, S.M. Auerbach, R.F. Lobo, G.W. Huber, J. Catal. 279 (2011) 257–268.
[28] J. Weitkamp, ChemCatChem 4 (2012) 292–306.
[29] K. Katō, Agric. Biol. Chem. 31 (1967) 657–663.
[30] R.S. Assary, L.A. Curtiss, Energy Fuels 26 (2012) 1344–1352.
[31] C. Moreau, P. Faugeras, P. Rivalier, P. Ros, G. Avignon, Appl. Catal. A Gen. 145 (1996) 211–224.
[32] M. Bicker, D. Kaiser, L. Ott, H. Vogel, J. Supercrit. Fluids 36 (2005) 118–126.
[33] G.R. Akien, L. Qi, I.T. Horvath, Chem. Commun. (Camb.) 48 (2012) 5850–5852.
[34] Y. Qiao, C.M. Pedersen, Y. Wang, X. Hou, ACS Sustain. Chem. Eng. 2 (2014) 2576–2581.
[35] H. Kimura, M. Nakahara, N. Matubayasi, J. Phys. Chem. A 117 (2013) 2102–2113.
[36] B. Smit, Chem. Rev. 108 (2008) 4125–4184.
[37] A. Poursaeidesfahani, M.F. de Lange, F. Khodadadian, D. Dubbeldam, M. Rigutto, N. Nair, T.J.H. Vlugt, J. Catal. 353 (2017) 54–62.
[38] K.L. Ratikorn Netrabukkana, Gregory L. Rorrer, Ind. Eng. Chem. Res. 35 (1996) 458–464.
[39] http://www.iza-structure.org/databases/.
[40] M. Leon, T.D. Swift, V. Nikolakis, D.G. Vlachos, Langmuir 29 (2013) 6597–6605.
[41] T.D. Swift, H. Nguyen, Z. Erdman, J.S. Kruger, V. Nikolakis, D.G. Vlachos, J. Catal. 333 (2016) 149–161.
[42] M. Holtkamp, T. Waluga, S. Scholl, J. Non-Equilib. Thermodyn. 37 (2012) 247–272.
[43] V.A. Yaylayan, A.A. Ismail, S. Mandeville, Carbohydr. Res. 248 (1993) 355–360.
[44] V.A. Yaylayan, A.A. Ismail, Carbohydr. Res. 276 (1995) 253–265.
[45] T. Barclay, M.G. Markovic, M.R. Johnston, P. Cooper, N. Petrovsky, Carbohydr. Res. 347 (2012) 136–141.
[46] T.D. Swift, C. Bagia, V. Choudhary, G. Peklaris, V. Nikolakis, D.G. Vlachos, ACS Catal. 4 (2013) 259–267.
[47] Y.R. Leshkov, M. Moliner, J.A. Labinger, M.E. Davis, Angew. Chem. Int. Ed. 49 (2010) 8954–8957.
[48] J.M. Carraher, C.N. Fleitman, J.P. Tessonnier, ACS Catal. 5 (2015) 3162–3173.
[49] D. Carnevali, O. Guévremont, M.G. Rigamonti, M. Stucchi, F. Cavani, G.S. Patience, ACS Sustain. Chem. Eng. 6 (2018) 5580–5587.
[50] L.W. Bao, H. Luo, L.Z. Kong, S.G. Li, W. Wei, Sun Y.H, ChemSusChem 10 (2017) 3040–3043.
[51] M. Wang, C. Liu, X. Xu, Q. Li, J. Anal. Appl. Pyrolysis 120 (2016) 464–473.
[52] Y. Wang, G. Ding, X. Yang, H. Zheng, Y. Zhu, Y. Li, Appl. Catal. B: Environ 235 (2018) 150–157.